AIAA JOURNAL
Vol. 48, No. 2, February 2010

Effect of Cell Geometry on Energy Absorption of Honeycombs Under In-Plane Compression

Bilim Atli-Veltin* and Farhan Gandhi†
Pennsylvania State University, University Park, Pennsylvania 16802

DOI: 10.2514/1.45021

This study examines the energy absorption capabilities of cellular honeycombs subjected to in-plane compression. ABAQUS nonlinear finite element analysis is used and cellular honeycombs with different cell geometries are considered. Simulation results are validated against previously published results for 30 deg cellular honeycombs. For various cell angles, comparison of simulation results for full-size honeycombs and their single-cell analogs suggest that the energy absorption can be accurately determined using the single-cell model. Results indicate that for cells with equal wall length, the specific energy absorption capability increases with increasing cellular honeycomb angle. A cell wall length study shows that the specific energy absorption (energy absorption per unit mass) is higher for cells with shorter vertical walls. A cell wall thickness study shows that increasing wall thickness increases the specific energy absorption. A vertical wall thickness study shows that the vertical walls should be thick enough not to buckle, but no thicker, providing the maximum energy absorption for minimum weight. A detailed analysis of cell deformation for different honeycombs and an insight of the underlying physics behind the differences in energy absorption capabilities observed for the different honeycombs are also presented.

Nomenclature

a	=	ratio of preyield modulus to the postyield modulus
b	=	cell depth
E	=	preyield modulus
h	=	height of the vertical wall
l	=	length of the inclined wall
t_h	=	thickness of the vertical wall
t_l	=	thickness of the inclined wall
α	=	cell wall length ratio; ratio of h to l
β	=	cell wall thickness to length ratio; ratio of t_l to l
η	=	cell wall thickness ratio; ratio of t_h to t_l
θ	=	cell angle; the angle between the inclined cell wall and horizontal direction
σ	=	stress

I. Introduction

ENERGY-ABSORBING applications convert the kinetic energy that the vehicle possessed before the crash to other forms of energy by undergoing large plastic deformations at steady force level. Ideal crushing behavior should have a steady load level for a large amount of stroke to absorb as much energy as possible while keeping the load levels below the tolerance of the human body [1,2]. Crushing of honeycombs generate this desirable form of energy absorption. Studies show that in-plane (along the edge direction) and out-of-plane (along the depth direction) crushing of honeycombs do not generate high initial peak loads and there is a plateau load corresponding to a large stroke [3]. In the case of out-of-plane direction loading, the honeycomb walls behave like thin wall panels; they buckle and fold over progressively [4]. In the case of in-plane direction loading, crushing of the honeycomb rows over each other provides the required continual form of deformation.

The energy-absorbing capability of honeycombs has been used in energy-absorbing applications since the 1960s, such as in the landing struts of the lunar landing spacecraft Surveyor [4]. The majority of the studies reported in the literature focus on the out-of-plane crushing of honeycombs. Sandwich structures, which consists of honeycomb core and facesheets, absorb energy when they are crushed, and their out-of-plane direction crushing behavior has been studied extensively [5–8]. In 1961, McFarland conducted an extensive study to determine an analytical expression for the out-of-plane crushing stress of hexagonal cells [9]. The effect of cell shape and foil thickness on out-of plane crush behavior has been studied by Yamashita and Gotoh [10]. However, the study presented in this paper focuses on the in-plane crushing of honeycombs.

For in-plane crushing of cellular honeycombs, in 1988, Klintworth and Stronge [11] developed fundamental theoretical models. In 1994, Papka and Kyriakides [12] presented their study on the in-plane crushing response of the honeycombs using ABAQUS finite element method analysis and compared their analytical results with experiments. In 1997, more theoretical work was presented by Gibson and Ashby [3]. In 2002, Honig and Stronge [13,14] presented theoretical, computational, and experimental results for in-plane crushing of honeycombs. Also in 2002, Chung and Waas [15] studied the biaxial static and dynamic in-plane crushing of circular honeycombs. Even though researchers presented experimental, theoretical, and numerical studies for in-plane crushing behavior of hexagonal or circular honeycombs, the effects of different cell geometries on in-plane crushing behavior of hexagonal honeycombs has not been explored. Previous studies not specifically focused on honeycomb crushing have already shown that cell geometry has a very large effect on the mechanical properties [16].

The purpose of the present study is to examine the effect of cell geometric parameters on the energy absorption during in-plane crushing of the cellular honeycombs, and to understand the underlying physics governing the difference in behavior for different cell geometries. The study starts with validating simulation results of regular hexagons (cell angle $\theta = 30$ deg) against previously published results. The validation is followed by investigating the sufficiency of simulating a unit cell of a full-size honeycomb core instead of the whole section. This is followed by comparing the energy absorption of honeycombs with different geometric parameters such as cell angles θ, cell wall length ratios $\alpha = h/l$, cell wall thickness to length ratio $\beta = t_l/l$, and cell wall thickness ratios $\eta = t_h/t_l$.

Presented as Paper 1881 at the 49th AIAA/ASME/ASCE/AHS/ASC Structures, Structural Dynamics, and Materials Conference, Schaumburg, IL, 7–10 April 2008; received 17 April 2009; revision received 15 September 2009; accepted for publication 16 September 2009.

*Ph.D. Candidate, Aerospace Engineering Department, 229 Hammond Building. Member AIAA.

†Professor, Aerospace Engineering Department, 229 Hammond Building. Senior Member AIAA.

The physical differences in these conditions that result in an increase or decrease in energy absorption are also highlighted for each geometry. This study will provide a basis for an optimization study to design lightweight cellular structure with better energy-absorbing capability. This paper not only provides a modified cell geometry that exhibits higher specific energy absorption but also highlights the physical crushing behavior that changes with changing geometric parameter.

II. Methodology

The in-plane crushing of honeycombs with hexagonal cells is conducted using ABAQUS finite element code version 6.7, which is a finite element program designed to be used in more advanced, generally nonlinear applications [17]. Honeycomb crushing has geometric nonlinearity (due to large deformations), material nonlinearity (due to bilinear behavior of the material), and the nonlinearities introduced due to the changing boundary conditions with contact of the opposing faces. These nonlinearities create a computationally expensive simulation problem. An effective way to reduce the computational cost is to simulate the crushing of a unit honeycomb section that represents a bigger honeycomb core. To find a unit honeycomb cell that represents the whole honeycomb core, it was decided to conduct the crushing simulations of a whole honeycomb core as well as a single cell. This preliminary study is followed by investigating the effect of each geometric parameter on energy absorption by crushing of unit cells with different cell angles, cell wall length, and thicknesses. The results are compared to find the geometric shape that provides the highest specific energy absorption.

A. Finite Element Model of a Single Honeycomb Cell

ABAQUS finite element method analysis is used to quasi-statically crush single cell (referred to as a "microsection" by Papka and Kyriakides [12]) and multicell honeycombs. Single-cell and multicell results are compared in the results section to verify the use of unit cell in the simulations instead of a whole honeycomb section to save computational time. These results show that the single-cell results capture the crushing behavior of a full honeycomb.

Figure 1 shows a single cell of hexagonal honeycomb core, which is the unit cell used in the simulations. It consists of eight inclined walls, two full length vertical walls, and, due to symmetry, six half-length vertical walls. The hexagon cells with 30 deg cell angle and equal wall lengths are called regular hexagonal honeycombs. The most common honeycomb manufacturing technique is called the "expansion" technique and it involves gluing sheets of virgin material at specific locations and expanding afterward. The glued section constructs the vertical walls. Therefore, the vertical walls have the double thickness of the inclined walls. In the single-cell model, the top and bottom short vertical walls have half the height of the long vertical walls due to symmetry, and the outer short vertical walls have half their actual thickness. Further, in the single-cell model, some boundary and symmetry conditions are required to suppress the rigid body motion. Vertical displacements of nodes a, b, and c, and horizontal displacement of b, are constrained. Rotations of nodes d, e, and f are matched to those at nodes a, b, and c, respectively. Loading is created by imposing downward vertical displacements of equal magnitudes on nodes d, e, and f.

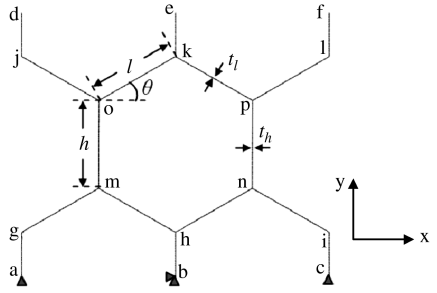

Fig. 1 Hexagonal honeycomb geometrical parameters and boundary conditions.

B22 beam elements are used to capture the movement of the walls. These elements follow Timoshenko beam theory and have three element nodes: one internal and two end nodes, each of them having 3 degrees of freedom, horizontal displacement, vertical displacement, and rotation. For the single cell, 2, 4, and 20 equal length elements are, respectively, used on the short vertical walls, long vertical walls, and on the inclined walls. This selection is based on the results of a convergence study.

Crushing of a single cell without any interaction property defined determines which walls need contact properties. For a single-cell simulation, seven self-contact conditions are defined; one is for the contact of the inner six walls of the hexagon, two of the conditions are defined for the right and left outer sides of the walls, and the last four are defined for the contact of the short vertical walls to the inclined walls. The normal behavior of the contact has a pressure-overclosure modification, which allows the pressure to increase exponentially as the surfaces come into contact.

The design parameters that determine the hexagon geometry are (as shown in Fig. 1) the vertical wall length h, the inclined wall length l, thickness of the vertical walls t_h, thickness of the inclined walls t_l, the cell angle θ, which is the angle between horizontal direction and the inclined walls, and the cell depth b. In the parametric study, nondimensional quantities relating these geometric parameters are used. These parameters are cell wall length ratios $\alpha = h/l$, cell wall thickness to length ratio $\beta = t_l/l$, and cell wall thickness ratios $\eta = t_h/t_l$.

The preliminary work of validating existing results starts with crushing a single-cell regular hexagon ($\theta = 30$ deg, $h = l$). If there is no imperfection on the geometry, the crushing is uniform, which means that the vertical walls do not tilt but compress. Experiments show that in real cases the crushing is not actually uniform, but the vertical walls tilt causing the rows to fold over each other. Because there will always be some imperfections in the manufactured honeycomb core, a misalignment imperfection is applied to the simulations. Therefore, the vertical walls of the single honeycomb cell (walls between nodes mo and np in Fig. 1) had a misalignment of 0.2 deg (in the original case, the vertical walls are considered to be on the 0 deg line). In the results section, it is shown that for small angles, the degree of imperfection does not have any effect on the crushing behavior. The unit cell is also used in the postyield modulus study, where the effect of postyield modulus on crushing behavior is investigated and the results are presented in the results section.

B. Finite Element Model of Honeycomb Core with Multiple Cells

Simulation of a single-cell honeycomb is followed by simulating the crushing of 9×6 (9 rows by 6 columns) honeycomb core. An undeformed multicell honeycomb can be seen in Fig. 2 with applied

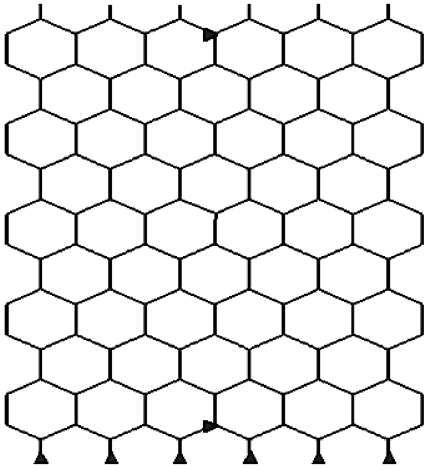

Fig. 2 Full-scale honeycomb core geometrical parameters and boundary conditions.

Table 1 Simulation matrix for cell angle study

	Cell angles			
Core size	15 deg	30 deg	45 deg	60 deg
Single cell	√	√	√	√
1 × 6	√	√	√	√
3 × 6	√	√	√	√
5 × 6	√	√	√	√
9 × 6	√	√	√	√

boundary conditions. As with the single-cell simulations, the vertical displacements of the bottom nodes are constrained to suppress the rigid body motion. Horizontal displacements of two nodes, one bottom and one top, are constrained to model the effect of friction along external contact surfaces. Honig and Stronge [13] used these boundary conditions to generate similar boundary conditions to dynamic crushing conditions. They concluded that the static loading study with these defined conditions is nearly identical to a model with contact surfaces.

The imperfection in a full-size honeycomb core is imposed on the vertical wall of the middle cell (fifth row, vertical wall common to third and fourth cells in the case of a 9 × 6 honeycomb core). Similar to the single-cell simulations, interaction properties are defined for the walls that are anticipated to contact. Self-contact interaction properties are defined for interior surfaces of all cells and exterior surfaces of right and left outer sides. In the cell angle study, multicell honeycombs are used as well as single-cell honeycomb. One of the observations as a result of the core size study was that the unit cell crushing simulations represents the crushing behavior of a multicell honeycomb (as long as the geometric parameters are same). Therefore, for the rest of the parametric study ($\alpha = h/l$, $\beta = t_l/l$, $\eta = t_h/t_l$), only the unit cell simulations are conducted. The test matrix for the call angle study is presented in Table 1.

III. Results

The best way to justify the simulation technique is to rerun some already studied cases and compare the results. As a result of an extensive literature survey study, Papka and Kyriakides's paper [12] on in-plane crushing of honeycombs is taken as a base paper. Therefore, the simulations presented in this study are based on the geometric and material parameters from Papka and Kyriakides's paper [12]. In single- and multicell honeycomb simulations, and for the cell angle study, vertical and inclined cell walls have an equal length of $h = l = 5.5$ mm. Inclined walls have a thickness of $t_l = 0.145$ mm, vertical walls have a double thickness of $t_h = 0.290$ mm, and the cell depth is $b = 10$ mm. For the cell wall length study, where $\alpha = h/l$ had various values, inclined wall length l was kept constant at 5.5 mm and h was varied. For the cell wall thickness study (effect of η), t_l was kept constant at 0.145 mm and t_h was varied. During the variation of $\beta = t_l/l$, η was kept constant at two. The material used in the simulations is aluminum, Al-5052-H39. The stress-strain behavior is assumed to be bilinear with preyield modulus of 68.97 GPa and yield stress of 292 MPa. The modulus beyond the yield point is defined by E/a; E is Young's modulus in the elastic region (preyield), and the parameter a, which defines the postyield modulus, is taken to be 100. Therefore, the postyield modulus of AL-5052 is estimated to be 689.7 MPa [12].

The resisting force that the structure generates over a stroke when it is crushed can be represented with a force vs displacement or a stress vs global strain curve. The area under the force vs displacement curve gives the total energy absorbed and the area under the stress vs strain curve gives energy absorbed per unit volume [4,18,19]. Specific energy absorption (SEA) is defined as the energy absorbed per unit mass. Stress is the total reaction force per effective cross section area and the global strain is the crushed displacement of the honeycomb compared to the total length of the uncrushed honeycomb [12]. Therefore, higher plateau stress for a longer stroke provides higher energy absorption.

A. Typical Crushing Behavior for Perfect and Imperfect Cells, and Effect of Imperfection

Figure 3 shows the crushing behavior of a honeycomb unit cell and several deformed cell shapes corresponding to various strain locations. Typically, when honeycombs made out of ductile materials, such as aluminum, are crushed, three regions appear on the stress vs strain plot: the initial linear elastic region, followed by the plateau region, and finally the steep "densification" region [3]. Gibson and Ashby [3] explain these regions as follows: In the initial linear region, until a critical stress is reached, stress increases linearly with increasing strain. When plastic hinges develop on the inclined walls, the linear elastic behavior ends, and the plateau region starts. The region called densification follows the plateau region. In the densification region, stress increases rapidly due to the contact of the opposing walls. Even though this explains the general compressive behavior of honeycomb crushing, changes in the material properties and geometric parameters result in differences in the output, such as higher or lower plateau stresses, or smaller or larger deformation (stroke).

Imperfections in the geometry cause a different mode of crushing where rotations of vertical walls take place, causing a delay of the densification region, as shown in Fig. 3b. Imperfections in the simulations are introduced by misalignment of the vertical walls. The deformation in the perfect case (Fig. 3a) is uniform until the end of the densification and the upper and lower walls come in contact around 70% global strain value (global strain value may change for a multicell honeycomb). In the case of an imperfect cell, uniform crushing ends when the plateau region starts, the vertical walls rotate, and densification occurs at higher global strains (Fig. 3b).

There are several ways to introduce imperfection to the honeycomb, such as variation on the wall thicknesses and wall lengths. In this study, an initial vertical wall misalignment is used. Effect of initial misalignment of the vertical walls on the stress-stain plot is also studied for 0.1, 0.2, 1, 2, and 4 deg initial misalignments. This is the angle between a vertical axis and the long vertical walls. Figure 4 shows the stress vs global strain curves of crushing of imperfect 30 deg single-cell honeycomb with different initial vertical wall misalignments. There is no significant effect of the misalignment angle on the plateau stress levels. To be consistent with Papka and Kyriakides [12], the remaining of the imperfect simulations has 0.2 deg of vertical wall misalignment.

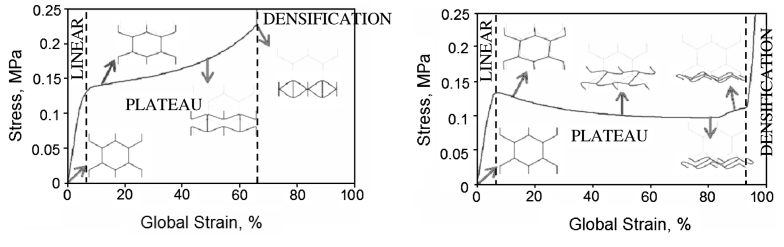

a) b)

Fig. 3 Compressive behavior of a) perfect and b) imperfect 30 deg honeycomb single-cell model.

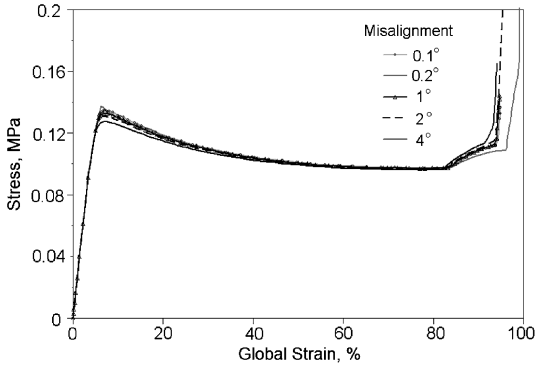

Fig. 4 Crushing behavior of single-cell model 30 deg imperfect honeycomb with different misalignment angles.

B. Validation Study

Validation study results are shown in the following figures. Figure 5 shows the stress vs global strain (stroke) plot of the crushing behavior for elastic and elastic-plastic material using a single-cell model (30 deg cell angle). It also shows the differences between a perfect honeycomb crushing (no misalignment) and an imperfect honeycomb crushing (0.2 deg misalignment). In the perfect case, the cell with elastic material follows the 0-A-B' line, whereas in the imperfect elastic case, it follows the 0-A-B line. For elastic-plastic material, perfect crushing follows the curve 0-a-b-c' and, for imperfect elastic-plastic, it follows the 0-a-b-c curve. Figures 5a and 5b compare the results of Papka and Kyriakides [12] to the present results, establishing the validity of the current simulations. In the case of elastic-plastic material, the plateau region starts at the same stress value for both perfect and imperfect cell, however, there is a stress relaxation in the imperfect case. The same stress relaxation in the imperfect simulation is also noticeable in Fig. 3b when compared with 3a.

A study of effect of postyield modulus on the compressive response of the single-cell model is conducted, and the results are plotted in Fig. 6. Figure 6a shows the plot from Papka and Kyriakides [12], and Fig. 6b shows the current simulation result. Again, the results are in good agreement.

Figures 5 and 6 verify our simulation technique for a single honeycomb cell. Figure 7 shows the crushing simulation of a 9×6 cell regular hexagonal honeycomb, from Papka and Kyriakides [12] (Fig. 7a) and current simulation results (Fig. 7b). These figures are

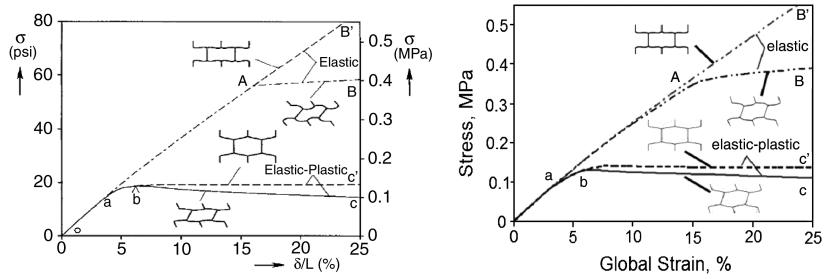

a) b)

Fig. 5 Crushing behavior of an elastic and elastic-plastic 30 deg single-cell honeycomb with and without misalignment: a) Papka and Kyriakides's results [12] and b) current simulations.

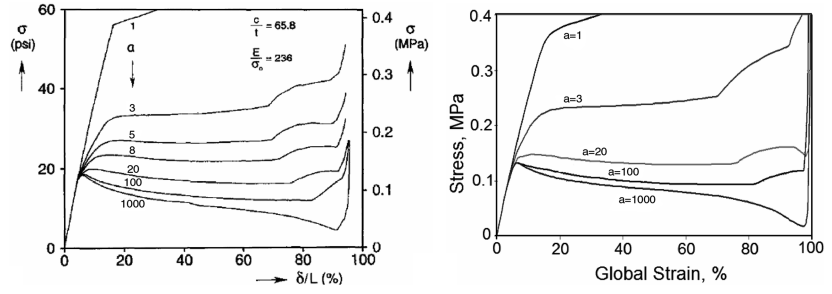

a) b)

Fig. 6 Effect of postyield modulus on crushing response of 30 deg single-cell regular honeycomb: a) Papka and Kyriakides's results [12] and b) current simulations.

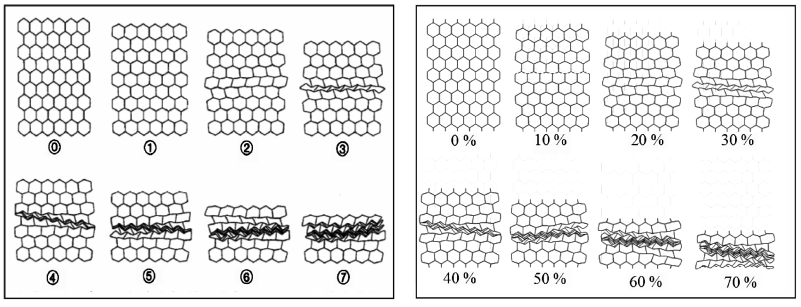

a) b)

Fig. 7 Crushing of a regular hexagon 9 × 6 cell honeycomb core: a) Papka and Kyriakides's results [12] and b) current simulations.

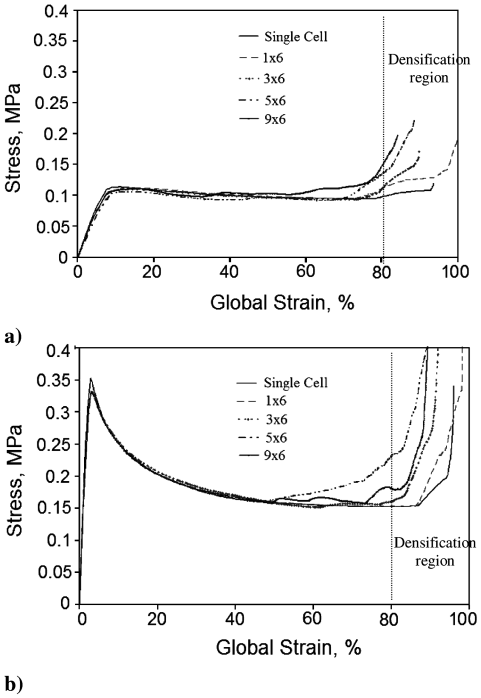

Fig. 8 Single-cell, 1 × 6 (1 row, 6 columns), 3 × 6, 5 × 6, and 9 × 6 results for a) 15 deg honeycomb and b) 60 deg honeycomb.

plotted to show that the crushing of the full honeycomb has the same general trend of band initiation and propagation (collapse of successive rows of cells).

C. Cell Core Size Study: Sufficiency of Simulating a Unit Cell

Figures 5–7 establish the validity of the current simulation results by comparison with the results previously published by Papka and Kyriakides [12]. The validation study is followed by crushing of hexagonal cells with different cell numbers and different cell angles. Figure 8 shows the stress vs global strain plots of 15 and 60 deg honeycomb simulations for single cell, 1 × 6 (1 row, 6 columns), 3 × 6, 5 × 6, and 9 × 6 core sizes. It can be seen that the plateau stresses obtained by simulating single cell or larger core sizes are very close. Although the global strain values at which the densification starts shows slight variation with honeycomb core size, for all cases it is beyond 80% global strain. While comparing energy absorption capability of various honeycombs (to construct Figs. 9b and 9c), a maximum global strain of 70% is used in the calculations. Therefore, simulating the crushing of a single cell instead of a larger core size is sufficient (if the exact global strain value where the densification occurs is not required), and this can result in a significant savings in computational time. The same study is also conducted for honeycombs with 30 and 45 deg honeycombs; however, results for 15 and 60 deg honeycombs are presented here as representative cases.

D. Effect of θ on Energy Absorption: Cell Angle Study

Figure 9a shows the stress vs global strain plot for honeycombs with 15, 30, 45, and 60 deg cell angles. These simulations are conducted using a single-cell model because the sufficiency of modeling a single cell instead of a full-size honeycomb is verified as shown in Figs. 8a and 8b. In all cases, densification starts around 90% global strain. It is apparent that the plateau stress for the 15 deg honeycomb is very close to that for the 30 deg honeycomb; whereas 45 and 60 deg honeycombs have higher plateau stresses. An initial load peak starts to appear on the stress curve for larger cell angles. Figure 9b shows the areas under the curves in Fig. 9a up to a global strain of 70%. The area under the stress vs global strain curve gives the total energy absorbed per unit volume (the total energy absorbed divided by the volume occupied by the undeformed honeycombs). It is seen that the 45 deg honeycomb can absorb 23% more and the 60 deg honeycomb can absorb 75% more energy per unit volume than the 30 deg honeycomb (baseline). The energy absorbed by the 15 deg honeycomb is 10% less than in the 30 deg case. Figure 9c shows the total energy absorbed per unit mass. These values are obtained by dividing the total energy absorbed by crushing a single honeycomb cell by the mass of a single honeycomb cell. Note that the mass of all the honeycombs in Fig. 9a are the same. According to these results, the 45 deg honeycomb absorbs 14.5% more and the 60 deg honeycomb absorbs 26% more energy per unit mass than the 30 honeycomb. The 15 deg honeycomb absorbs 15.7% less energy (per unit mass) than the 30 deg honeycomb. The 60 deg honeycomb appears to be the best with the highest absorbed energy per unit volume and with the highest absorbed energy per unit mass. However, the high initial peak stress of the 60 deg honeycomb could potentially be a cause for concern.

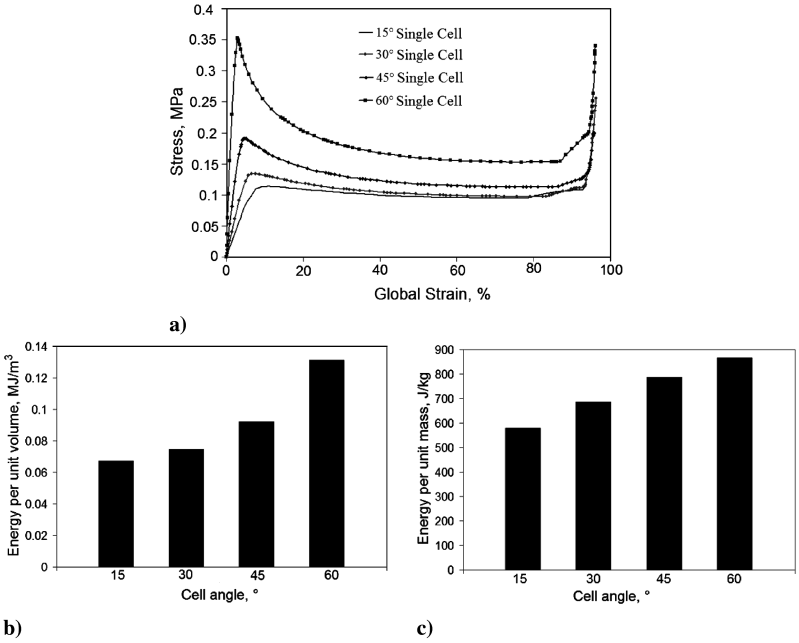

Fig. 9 Effect of cell angle on energy absorption: a) single imperfect cell crushing results for 15, 30, 45, and 60 deg honeycombs, b) energy absorbed per unit volume up to 70% global strain, and c) energy absorbed per unit mass up to 70% global strain.

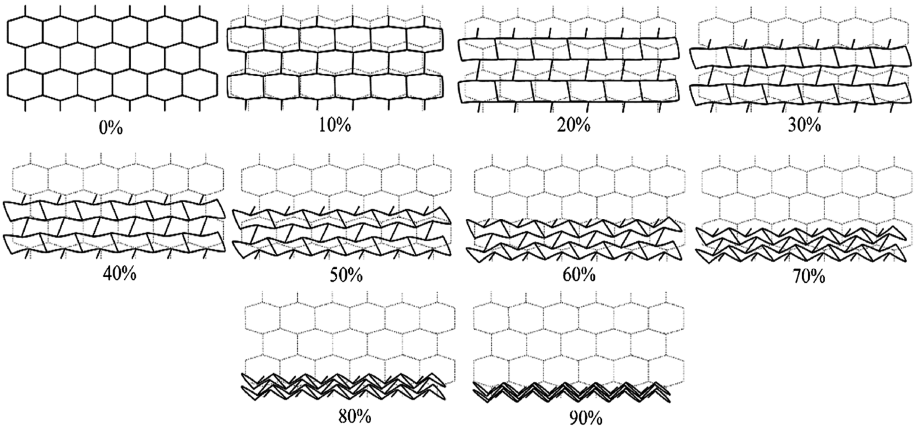

Fig. 10 Crushing of 3 × 6 honeycomb core with 15 deg cell angle.

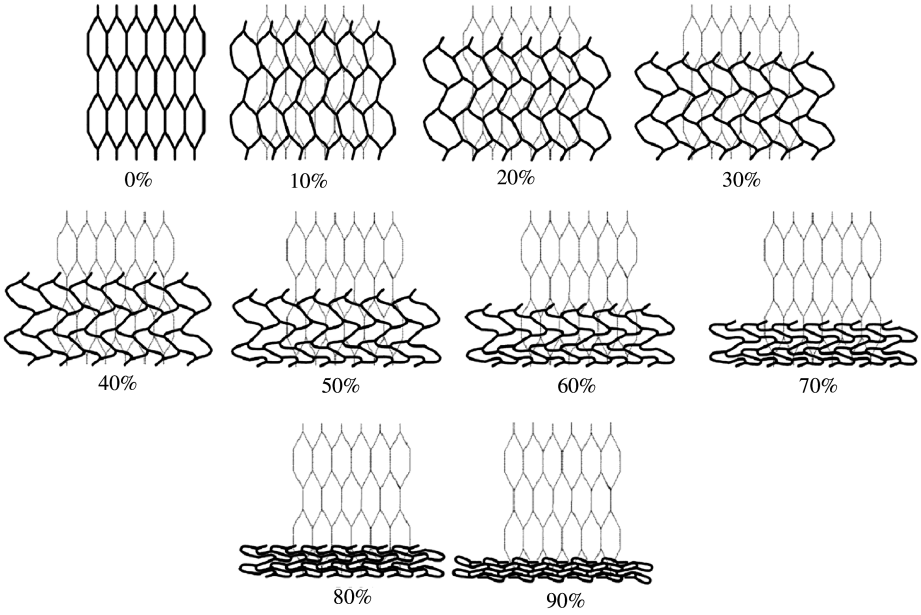

Fig. 11 Crushing of 3 × 6 honeycomb core with 60 deg cell angle.

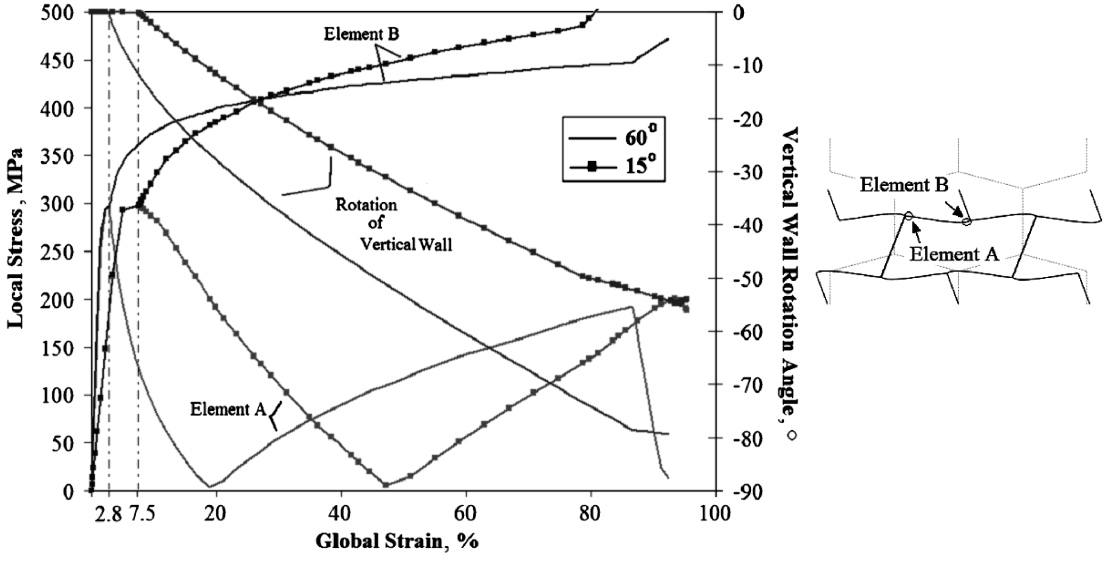

Fig. 12 Local Mises stresses at the ends of inclined walls (elements A and B), and rotation of the vertical wall for 15 and 60 deg honeycombs.

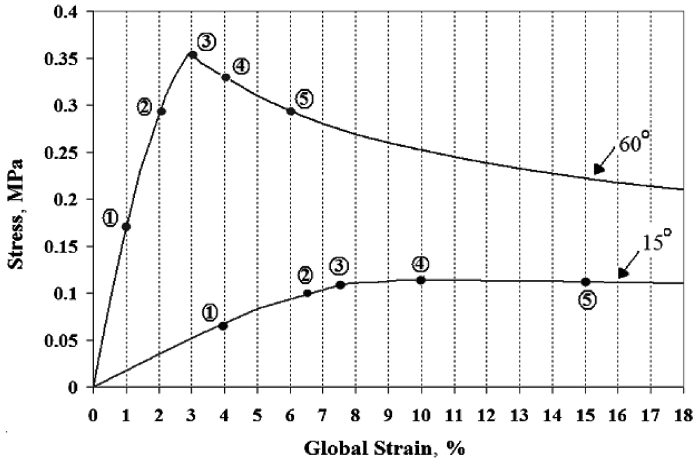

a)

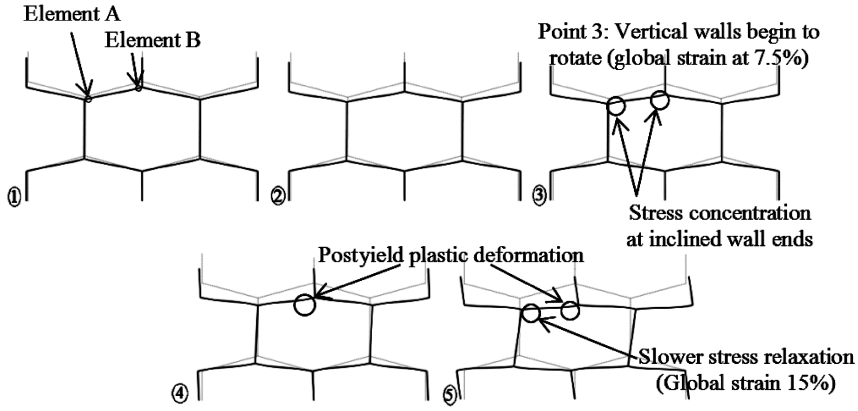

b)

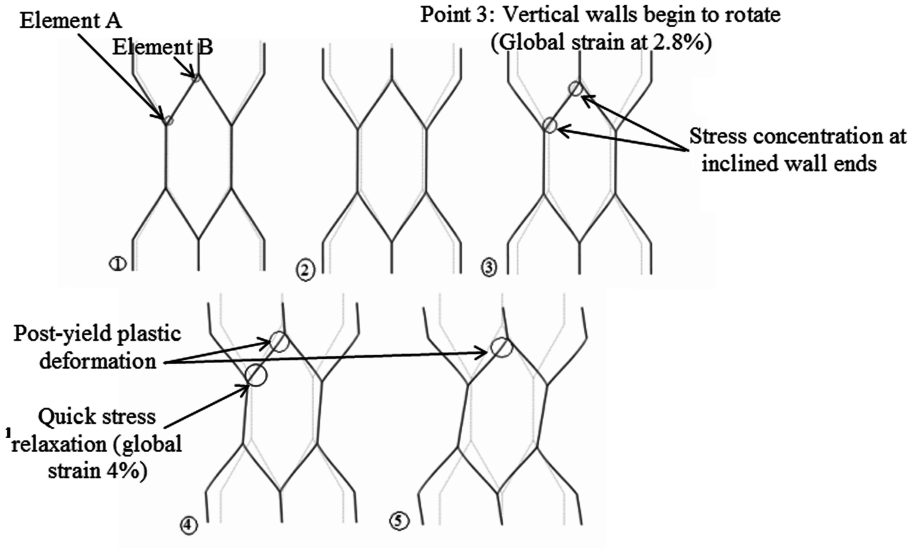

c)

Fig. 13 Effect of cell angle on cell deformation: a) global stress vs strain curve for 60 and 15 deg single cells, up to 18% global strain (circled numbers correspond to the deformed configurations in Figs. 13b and 13c), b) cell wall deformations for 15 deg, and c) cell wall deformations for 60 deg.

E. Underlying Physics of Cell Angle Study

Figures 10 and 11 show the deformed and undeformed configurations of honeycombs with 3×6 core sizes for 15 and 60 deg cell angles, respectively. It is observed that during crushing, inclined walls of 60 deg honeycomb develop much more bending than the 15 deg honeycomb. In the case of the 15 deg honeycomb, a localized hinge develops where maximum bending occurs and the rest of the inclined wall rotates around that hinge as a rigid body. However, in the case of the 60 deg honeycomb, bending in the inclined wall is not localized, but distributed. Therefore, the inclined walls do not behave as a rigid body undergoing pure rotation about a hinge.

Vertical wall rotations are also different for these two cases. For the same global strain value, the rotation of the vertical walls of the 60 deg honeycomb are much larger than the 15 deg honeycomb

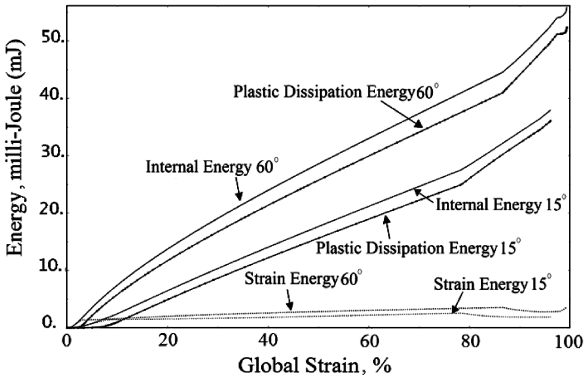

Fig. 14 Internal energy of an inclined wall of a single cell and contributing energies of plastic dissipation and strain energy for 15 and 60 deg cell angles.

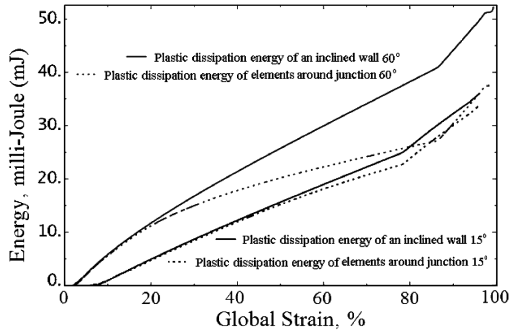

Fig. 15 Plastic dissipation energies of inclined wall of a single cell (summation of energies of 20 elements along the edge), and energies of the four elements (closest to the hinge) for 15 and 60 deg cases.

vertical walls, which is also clearly seen in Fig. 12. Figure 12 also shows the local stresses in elements A and B, which are located at the ends of the inclined walls, for 15 and 60 deg single-cell honeycombs. It can be seen that when the vertical walls start to rotate (at 2.8% global strain for the 60 deg honeycomb and 7.5% global strain for the 15 deg honeycomb), local stress in element A decreases while that in element B increases. Stress relaxation in element A is much sharper for the 60 deg honeycomb than the 15 deg honeycomb. Also note that at the point where the vertical walls start to rotate and element A starts to show stress relaxation behavior, a plastic hinge starts to develop around element B. This point corresponds to the initial peak on the stress vs global strain curve (as shown in Fig. 9a).

Figure 13a presents the stress vs global strain for the 15 and 60 deg honeycombs. Figures 13b and 13c show the deformation of a single cell for the 15 and 60 deg honeycombs, respectively, at different global strains. Point 3 in Figs. 13a–13c corresponds to the initiation of the vertical wall rotation. At this point, the local stress in element A has peaked and stress relaxation begins (seen in Figs. 12, 13b, and 13c). The sharper stress relaxation for the 60 deg case (compare Figs. 13b and 13c, also observed in Fig. 12) corresponds to a prominent initial peak followed by stress reduction on the global stress/strain curve in Fig. 13a. Such a prominent peak and subsequent stress reduction is absent for the 15 deg case where the local stress relaxation in element A is more gradual. Point 3 also corresponds to the initiation of plastic deformation in element B, resulting in the development of a hinge or a flexure.

The energy output of ABAQUS shows that the internal energy of the cell has two contributing components: the plastic dissipation energy and the strain energy. Figure 14 shows these energy components for 15 and 60 deg cells inclined wall (only one inclined wall) as a function of the global strain. It is clear that most of the energy is in plastic dissipation form, which is caused by the plastic deformation of the inclined walls.

Figure 15 presents the plastic energy for the entire inclined wall (20 elements) as well as for the section closest to the junction [four elements starting from element B (marked in Figs. 12, 13b, and 13c) and moving toward the center of the wall]. It is observed that for the 15 deg honeycomb, the plastic energy in the entire inclined wall is very close to the plastic energy in the elements near the junction. On the other hand, for the 60 deg honeycomb, the energy in the entire inclined wall is substantially larger than that in the end elements. This implies that there is a lot of localized curvature (formation of a concentrated hinge) at the end of the inclined wall for the 15 deg case. The curvature is more distributed for the 60 deg case, implying development of an extended flexure. This phenomenon is also observed in Fig. 11.

F. Effect of α on Energy Absorption: Cell Wall Length Study

The effect of cell wall length on energy absorption is studied by simulating crushing of 30 and 60 deg unit cells with different α values. In a regular honeycomb, $\alpha = 1$ because the vertical and inclined wall lengths are equal. Figure 16 shows the geometry of hexagonal cells for five different α values: for $\alpha = 2$, the vertical wall length is twice that of the inclined wall; $\alpha = 1$ shows a regular honeycomb; for $\alpha = 0.5$, the vertical wall length is half of the inclined wall lengths; and for $\alpha = 0.25$, the vertical wall length is a quarter of the inclined wall lengths. A diamond cell shape corresponds to $\alpha = 0$, where the vertical walls disappear. For these simulations, β and η values are not varied.

Figure 17 shows the stress vs global strain curves up to 80% global strain at various α values; Fig. 17a is for 30 deg and Fig. 17b is for 60 deg unit cells. For hexagonal cells, it is seen that the plateau stress decreases with increasing α for both 30 and 60 deg unit cells; however, when $\alpha = 0$, the diamond shape, the cell crushing generates a stress vs strain curve, which does not follow this trend. For the 30 deg cell, the diamond cells' plateau level is around the regular ($\alpha = 1$) cell levels, however, for the 60 deg cell, the diamond cells' plateau level falls around the $\alpha = 0.5$ levels. It is also observed that the initial peak load observed for hexagonal cell crushing disappears in the case of diamond cell crushing.

Figure 18 shows the energy absorbed per unit mass, SEA (Fig. 18a), and the energy absorbed per unit volume (Fig. 18b), for global strains up to 70%. For 30 deg cells, $\alpha = 0.25$ absorbs 2.4% more energy per unit mass than $\alpha = 1$. For 60 deg cells, $\alpha = 0.25$ absorbs 45% more energy per unit mass than $\alpha = 1$. The 60 deg, $\alpha = 0.25$ cell absorbs 88.6% more specific energy than the regular honeycomb cell ($\theta = 30$ deg, $\alpha = 1$). The energy per unit volume absorbed by the 60 deg cell with $\alpha = 0.25$ is 2.68 times higher than the regular honeycomb cell.

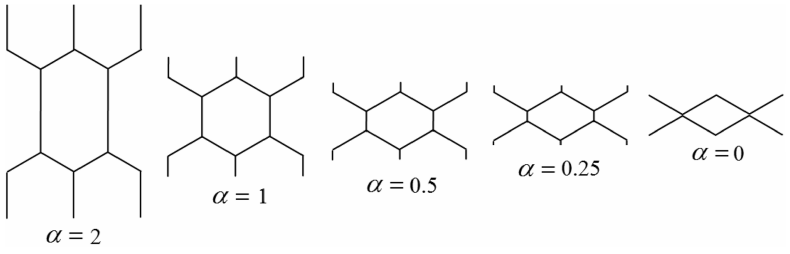

Fig. 16 Cell geometry at various α values ($\beta = \beta^*$, $\eta = 2$).

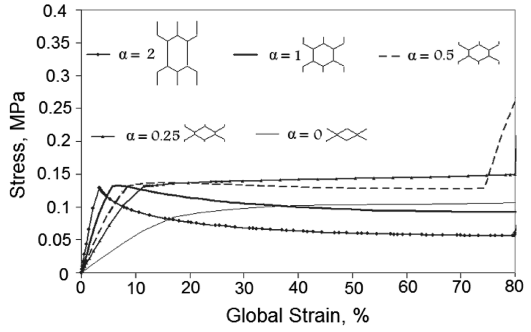

a)

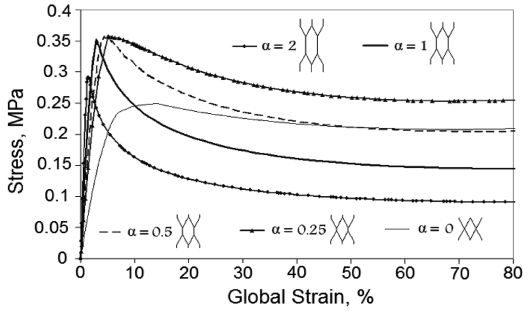

b)

Fig. 17 Global stress vs strain curves for a) 30 deg and b) 60 deg hexagonal unit cell at various α values.

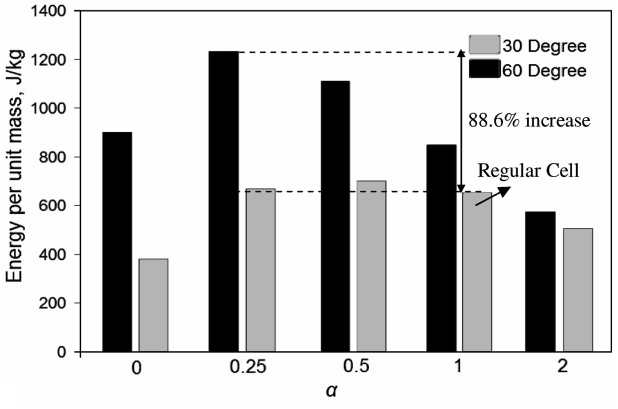

a)

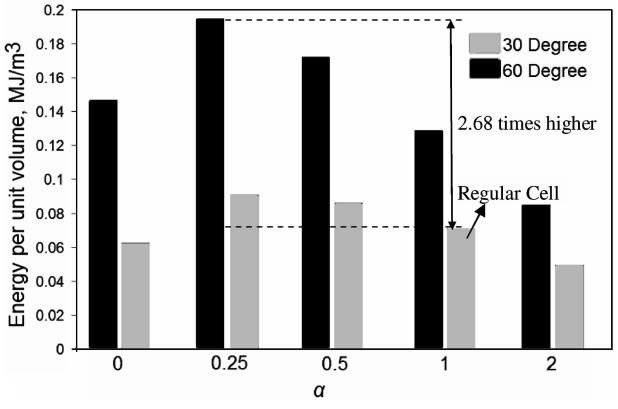

b)

Fig. 18 Energy absorbed a) per unit mass and b) per unit volume for 30 and 60 deg hexagonal unit cell at various α values (up to 70% strain).

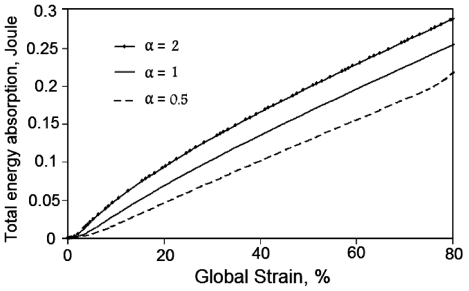

Fig. 19 Total energy absorption by a 30 deg honeycomb cell with different α values.

G. Observations and Underlying Physics of Cell Wall Length Study

Total energy absorbed by a 30 deg honeycomb cell is shown in Fig. 19 for different α values. Figure 20 shows the energy absorbed due to the plastic deformation in a single inclined wall (solid line, 20 elements) and the last four elements on the hinge end of the inclined wall (dashed lines). It can be seen that increasing α causes the dashed lines to separate from the solid lines, which implies that there is a more distributed deformation over the length of the inclined wall, rather than all the deformation concentrating around a virtual hinge point.

From Figs. 19 and 20, it can be seen that the actual energy increases when α increases (this is less for 60 deg, results not shown). Based on Fig. 20, this could be attributed to the rotation in the vertical walls and the initiation of the plastic deformation in the inclined walls starting at lower global strain for higher α. The lower energy per unit volume for higher α then is due to the larger volume associated with the higher α cells (see Table 2).

The initial slopes of the curves in Figs. 17a and 17b vary, showing that Young's modulus in the elastic region changes with α. The slope of these curves can be compared to analytical results, which can be calculated using the formula provided by Gibson and Ashby [3]. The formula that calculates Young's modulus of the honeycomb cell in the y direction (directions are shown in Fig. 1) is given in Eq. (1). Table 3 compares the slopes in Figs. 17a and 17b to Young's modulus calculated using Eq. (1). It can be seen that the variation of α affects Young's modulus, and simulation results match well to the formula. Increasing α increases Young's modulus of the honeycomb in the elastic region:

$$E_y = E_s \cdot \left(\frac{t_l}{l}\right)^3 \frac{h/l + \sin\theta}{\cos^3\theta} \tag{1}$$

Figure 21 shows the local stresses at the end elements (left and right) of an inclined wall for a 30 deg honeycomb cell at various α values. The thin solid lines correspond to the diamond shape ($\alpha = 0$), dashed lines correspond $\alpha = 0.5$, and lines with symbols correspond to $\alpha = 2$. Black lines show the left end where there is no hinge, because there is a stress relaxation beyond the initial linear region, and the gray lines show the right end element surface stresses where a hinge is generated, because a stress increase is observed beyond the initial linear region. In the case of the diamond shape cell, stress

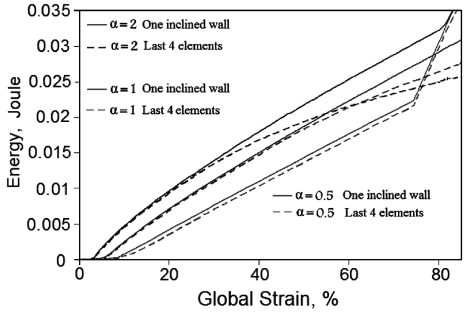

Fig. 20 Variation of plastic energy absorption along the elements of an inclined wall with varying α for a 30 deg cell.

Table 2 Volume and mass of 30 deg cells with various relative to the regular cell

	30 deg cell angle		
	$\alpha = 0.5$	$\alpha = 1$	$\alpha = 2$
Volume/volume of regular cell	0.66	1	1.66
Mass/mass of regular cell	0.75	1	1.5

Table 3 Comparison of Young's modulus (MPa) calculated and simulation results

	30 deg		60 deg	
α	Analysis, Eq. (1)	ABAQUS	Analysis, Eq. (1)	ABAQUS
2	4.23	4.42	25.20	25.2
1	2.54	2.74	16.41	15.7
0.5	1.69	1.85	12.01	12.9

curves overlap because both ends of an incline wall exhibit the same kind of deformation and increasing stress beyond the linear region indicates that a hinge forms at both ends, unlike a nonuniform cell deformation. As expected, because the deformation is uniform, the local stresses on the left and right elements coincide for the diamond shape cell (thin solid lines).

For nonzero α, as the vertical walls get shorter (decreasing α), the influence of the vertical walls on the deformation gets less, and therefore smaller local stress variation between the left and right end is observed in Fig. 21, where the local stresses on the no-hinge side of the inclined wall vary much more for the high α values compared to small α values.

From the global stress vs strain curves in Figs. 17a and 17b, it can be seen that the relaxation beyond the initial peak stress is higher for high α values. The similar relaxation is also observed in Fig. 21 where the local stresses significantly drop on the no-hinge end for cells with high α values. As the deformed cell shapes shown in Fig. 21 at 20 and 40% global strains for $\alpha = 2$ and $\alpha = 0.5$ indicate, the vertical wall rotation is higher for high α values, allowing the local stress relaxations on the no-hinge end (shown in Fig. 21). From these observations, it can be concluded that the relaxations on the global stress vs strain curve are linked to the local stress relaxations on the no-hinge end, which are caused by the vertical walls rotations.

H. Effect of β on Energy Absorption: Cell Wall Length to Wall Thickness Ratio Study

β is the ratio of the inclined wall thickness to the wall length. For the regular honeycomb simulations, these values were $t_l = 0.145$ mm and $l = 5.5$ mm, which gives the ratio of 0.026. This value is denoted as β^* and the variation of β is given by multiples of β^*. In this part of the study, two different β values are investigated in addition to the β^* for 30 and 60 deg unit cells. Figure 22 shows how unit cell geometry looks like for different β values. Other geometric nondimensional parameters are not changed; $\alpha = 1$ and $\eta = 2$. Figure 23 shows the effect of β on the global stress vs strain plot for 30 and 60 deg unit cells. The black lines correspond to the 60 deg cells and the gray lines correspond to the 30 deg honeycomb cells. It is seen that increasing wall thicknesses increases the energy absorption.

Figure 24 shows the corresponding SEA (Fig. 24a) and energy per unit volume (Fig. 24b) up to 70% global strain. The increase in the energy absorption can be found by comparing the values to the regular honeycomb, which is the cell with 30 deg cell angle and $\beta = \beta^*$. As can be seen in Fig. 24a, the 30 deg honeycomb with $2\beta^*$ absorbs 2.3 times more energy per unit volume compared to the regular honeycomb (30 deg cell angle and $\beta = \beta^*$). The 60 deg honeycomb with $2\beta^*$ absorbs 3.02 times more energy per unit volume compared to the regular honeycomb.

It can also be seen in Fig. 24b that the 30 deg honeycomb with $2\beta^*$ absorbs 4.71 times more energy per unit mass compared to the regular cell (30 deg cell angle and $\beta = \beta^*$). The 60 deg honeycomb with $2\beta^*$ absorbs 8.57 times more energy per unit mass compared to a regular honeycomb. These values show that increasing wall thickness results in higher specific energy absorption per unit volume and per unit mass.

I. Observations and Underlying Physics of Cell Wall Thickness Study

The energy absorption has two components; energy absorbed due to the plastic deformation and the strain energy. It was explained earlier that most of the energy absorption is due to the plastic dissipation energy caused by the deformation of the inclined walls. Table 4 shows the ratio of the energy absorbed by the plastic deformation to the total energy absorption for different β^* values. When these percentages are compared for different β^* values, it is seen that increasing wall thicknesses increases the plastic deformation energy. There is not a significant variation on the percentages for varying α.

Increasing wall thickness increases the surface strains and stresses on the cell walls causing more plastic deformation and therefore more energy absorption. The cell wall thickness can be increased until the surface strains exceed the strain levels at which the material

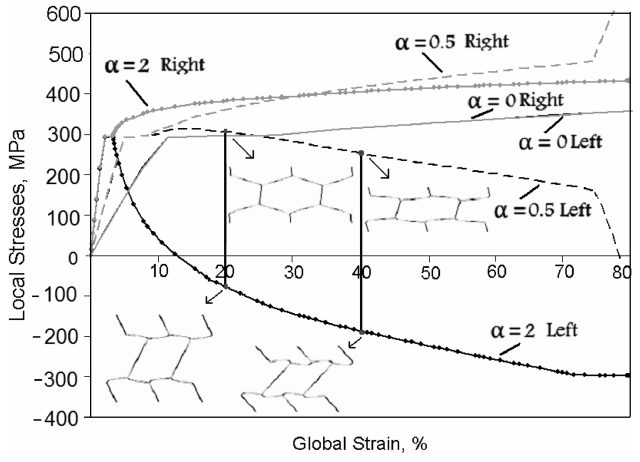

Fig. 21 Local stresses at the right (gray lines) and left (black lines) end elements of an inclined wall for a 30 deg cell for different α values.

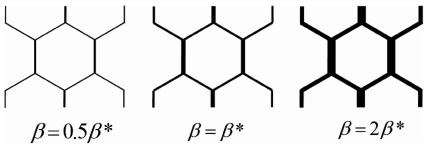

Fig. 22 Cell geometry at various β values ($\alpha = 1$, $\eta = 2$).

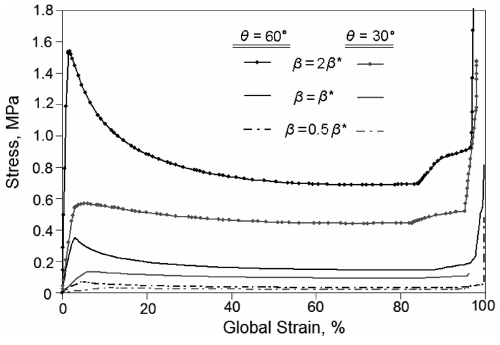

Fig. 23 Global stress vs strain curves for 30 and 60 deg hexagonal unit cell at various β values.

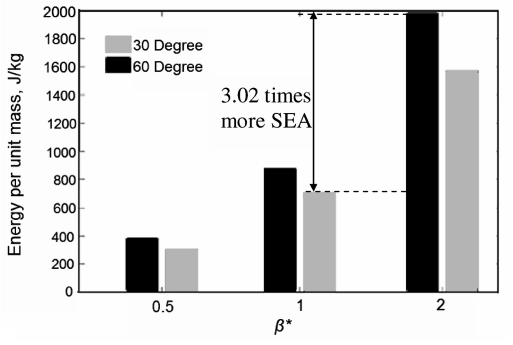

a)

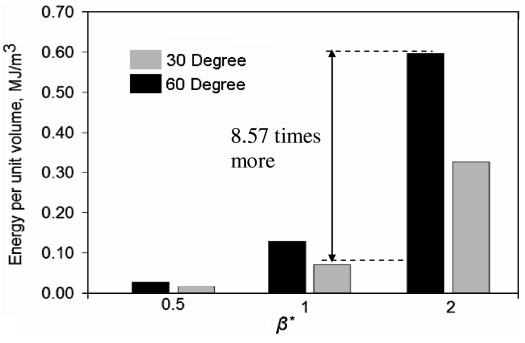

b)

Fig. 24 Energy absorbed a) per unit mass and b) per unit volume for 30 and 60 deg hexagonal unit cell at various β values (up to 70% strain).

fractures or ruptures. From Figs. 24a and 24b, it is also observed that an increase in the energy absorption with increasing wall thickness is greater for 60 deg honeycombs than for 30 deg honeycombs.

J. Effect of η on Energy Absorption: Cell Wall Thickness Study

The ratio of vertical to inclined wall thickness is η. The effect η on the energy absorption is studied by simulating crushing of 30 and 60 deg unit cells. In a regular honeycomb, due to the most common manufacturing method of expansion technique, vertical walls are assumed to have twice the thickness of the inclined walls, giving $\eta = 2$. In this study, several η values are investigated. Figure 25 shows the cell geometry corresponding to $\eta = 1$, 2, and 3. In this study, other geometric parameters are kept constant; $\alpha = 1$ and $\beta = \beta^*$.

Figure 26 shows the global stress vs strain plots for different η values. The black lines correspond to the 60 deg and the gray lines correspond to the 30 deg honeycomb cell. For both cases, it is seen that η does not have any significant effect on the crushing behavior for the three η values ($\eta = 1.5$, 2, 3) that are investigated. Figure 27 shows the SEA corresponding to these three η values. Even though the plateau stresses overlap on the global stress vs strain curve, SEA for smaller η values is greater than the higher η values. Because, as η increases, the energy absorption in the inclined walls remains unchanged but the thicker vertical walls increase the mass. Energy absorption per unit volume does not change for these values of η ($\eta = 1.5$, 2, 3) because the curves overlap.

Table 4 Ratio of plastic deformation energy to total energy absorption

β^*	30 deg	60 deg
0.5	0.843	0.852
1	0.911	0.917
2	0.945	0.947

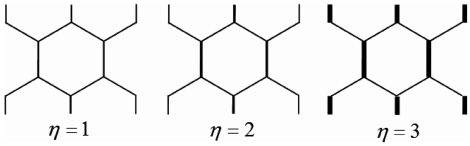

Fig. 25 Cell geometry at various η values ($\alpha = 1$, $\beta = \beta^*$).

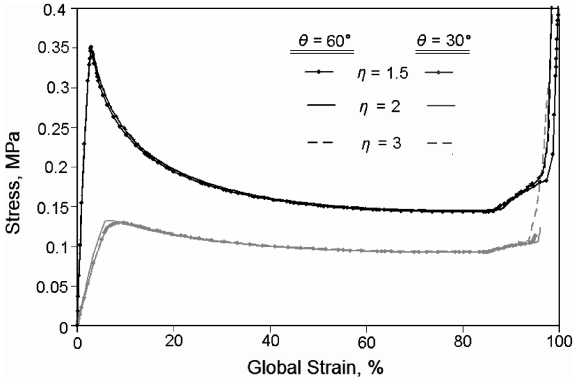

Fig. 26 Global stress vs strain curves for 30 and 60 deg hexagonal unit cell at various η values.

K. Observations and Underlying Physics of Vertical Wall Thickness Study

If η is reduced below a critical value, buckling of the vertical walls of the honeycomb cell initiates the crushing of the cell. This effect is studied for a 30 deg honeycomb cell, and the results are shown in Fig. 28. It is shown that for high η values, such as $\eta = 4$ and 2, there is no significant effect on the stress vs strain behavior. However, for small η values, crushing starts much earlier compared to the high η values, and the plateau stress is much lower, causing a significant reduction in the energy absorption. The optimum η value should be high enough to result in crushing due to bending of the inclined walls and low enough not to provide unnecessary weight. Figure 28 shows that for a 30 deg honeycomb cell, $\eta = 1$ can be used for determining the optimum vertical wall thicknesses for the modified cell geometry, which provides higher SEA compared to the honeycombs with regular cell.

L. Optimizing the Cell Design

In this study, honeycomb cell geometry with improved SEA relative to the regular honeycomb cell is suggested. This suggestion is based on the results of the trend studies. An optimization method was not followed due to the nonlinear characteristics of the problem. Results from the cell angle parametric study, cell vertical wall to inclined wall length ratio, cell wall thickness to length ratio, and vertical to inclined wall thickness ratio study presented in this paper show the following:

1) Increasing cell angle increases the specific energy absorption.

2) Decreasing vertical wall length increases the specific energy absorption.

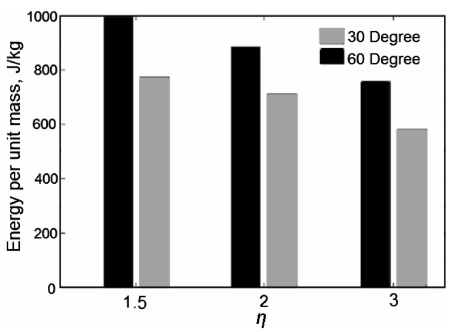

Fig. 27 SEA for a 30 and 60 deg hexagonal unit cell at various η values.

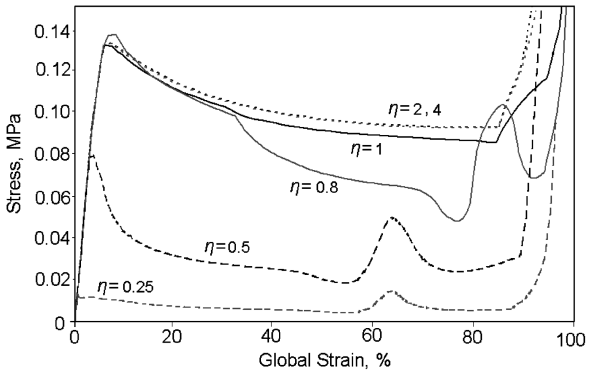

Fig. 28 Global stress vs strain curves for 30 deg hexagonal unit cell at various η values.

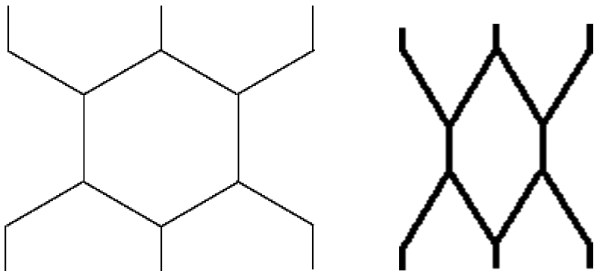

a) **b)**

Fig. 29 Honeycomb cell geometry: a) regular honeycomb and b) modified cell geometry with higher SEA.

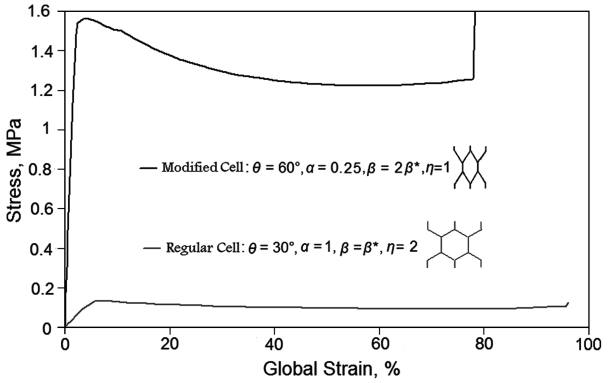

Fig. 30 Global stress vs strain curves for regular and modified-geometry hexagonal unit cells.

3) Increasing wall thicknesses increases the specific energy absorption.

4) Vertical wall thickness should be large enough to not cause buckling and early initiation of crushing.

These observations provide a modified design where the cell has a bigger cell angle, shorter and thinner vertical walls, and thicker inclined walls. Energy absorption of a cell with $\theta = 60$ deg, $\alpha = 0.25$, $\beta = 2\beta^*$, and $\eta = 1$ can be compared with SEA of a regular cell, which has $\theta = 30$ deg, $\alpha = 1$, $\beta = \beta^*$, and $\eta = 2$. The cell shapes can be seen in Fig. 29.

Figure 30 shows the crushing behavior of the modified-geometry and regular honeycomb cells that are shown in Fig. 29. The black line, which represents the modified cell geometry, shows a much higher plateau level compared to the regular honeycomb behavior, which is shown with the gray line. The area under the curves up to 70% global strain show that the modified cell geometry absorbs around 3151 J/kg energy per unit mass, which is 4.8 times higher than a regular cell. The modified cell also absorbs 0.89 MJ/m^3 energy per unit volume, which is 12.7 times higher compared to a regular cell.

IV. Conclusions

In this paper, simulation results of in-plane crushing of hexagonal honeycombs are presented. The effect of geometric parameters on the energy absorption is investigated. The material properties, cell geometric parameters, and imperfections are the same as the previous studies from Papka and Kyriakides [12]. The perfect hexagon ($\theta = 30$ deg, $h = l$) simulation results are validated against Papka and Kyriakides's results, and an examination of the behavior of honeycombs with various cell angles ($\theta = 15, 30, 45$, and 60 deg) is conducted. The energy absorption of the cells with different cell wall length ratios ($0 < \alpha < 2$), cell wall thickness to length ratio ($0.5\beta^* < \beta < 2\beta^*$), and vertical to inclined wall thickness ratio ($0.25 < \eta < 4$) are compared. The following conclusions are made:

1) For various cell angles, comparison of simulation results for full-size honeycombs and their single-cell analogs suggest that the energy absorption can be accurately determined using the single-cell model.

2) The cell angle study suggested that increasing cell angle increases the energy absorption significantly.

3) A localized deformation on the inclined cell wall was observed for cells with small cell angle as opposed to a more distributed deformation for the cells with higher cell angle.

4) Decreasing the vertical wall length increases the energy absorption per unit mass. It is also shown that a diamond cell shape, where the vertical walls disappear, does not have an improved energy absorption. Therefore, it is concluded that a short vertical wall results in highest energy absorption.

5) The total energy absorbed by a cell with long vertical walls is greater, however, the volume it occupies is greater and it weighs more relative to a regular cell. Therefore, the energy absorption per unit mass and unit volume is higher for cells with short vertical walls (small α).

6) The stress relaxation on the global stress vs strain curve for high α values is linked to the local stress drop on the no-hinge end of the inclined walls. The vertical wall rotations increase with increasing α, causing the local stresses to drop more for high α values.

7) The cell wall thickness study shows that increasing wall thickness increases the energy absorption. This result is expected because, during the crushing, inclined walls bend generating high stress levels on the wall surfaces. When the wall is thicker, the surface stresses and the plastic deformation get higher, providing better energy absorption. Increasing wall thickness is limited with the rupture strain limits of the material.

8) The vertical wall thickness study shows that when the thickness of the vertical walls reduces such that the critical buckling load of the vertical wall is lower compared to the maximum bending load of the inclined walls, buckling occurs earlier. Plots show that for the low levels of vertical wall thickness, the plateau loads are much lower compared to the case where the crushing initiates due to the yielding of the inclined walls. Provided the vertical walls are thick enough that they do not buckle, increasing the vertical wall thickness further did not change the crushing behavior. Therefore, it is suggested that vertical walls be thick enough not to buckle, but no thicker, providing the maximum energy absorption for minimum weight.

Acknowledgments

This material is based upon work supported by the U.S. Office of Naval Research under Award No. N00014-06-1-0205. Any opinions, findings, and conclusions or recommendations expressed in this publication are those of the authors and do not necessarily reflect the views of the Office of Naval Research.

References

[1] Cronkhite, J. D., and Berrry, V. L., "Crashworthy Airframe Design Concepts, Fabrication and Testing," NASA, CR 3603, 1982.

[2] U.S. Army Aviation Research and Technology Activity, "Aircraft Crash Survival Design Guide," Vol. 3, *Aircraft Structural Crash Resistance*, 1989, p. 21.

[3] Gibson, J. L., and Ashby, M. F., *Cellular Solids*, 2nd ed., Cambridge Univ. Press, Cambridge, Engand, U.K., 1997, Chap. 4.

[4] Brentjes, J., "Honeycomb as an Energy Absorbing Material," *AIAA/ASME 8th Structures, Structural Dynamics and Materials Conference*, AIAA, New York, March 1967, pp. 468–473.

[5] Goldsmith, W., and Sackman, J. L., "An Experimental Study of Energy Absorption in Impact on Sandwich Plates," *International Journal of Impact Engineering*, Vol. 12, No. 2, 1992, pp. 241–262. doi:10.1016/0734-743X(92)90447-2

[6] Moriarty, K., and Goldsmith, W., "Dynamic Energy Absorption Characteristics of Sandwich Shells," *International Journal of Impact Engineering*, Vol. 13, No. 2, 1993, pp. 293–317. doi:10.1016/0734-743X(93)90098-R

[7] Zhou, G., Hill, M., and Hookham, N., "Investigation of Parameters Governing the Damage and Energy Absorption Characteristics of Honeycomb Sandwich Panels," *Journal of Sandwich Structures and Materials*, Vol. 9, No. 4, July 2007, pp. 309–342. doi:10.1177/1099636207067134

[8] Wierzbicki, T., Alvarez, A. L., and Hoo, F. M. S., "Impact Energy Absorption of Sandwich Plates with Crushable Core," *American Society of Mechanical Engineers, Applied Mechanics Division*, Vol. 205, Applied Mechanics Div. Series, American Society of Mechanical Engineers, Fairfield, NJ, 1995, pp. 391–411.

[9] McFarland, R. K., "A Limit Analysis of the Collapse of Hexagonal Cell Structures Under Axial Load," Jet Propulsion Lab., California Inst. of Technology Technical Rept. 32-186, Dec. 1961.

[10] Yamashita, M., and Gotoh, M., "Impact Behavior of Honeycomb Structures with Various Cell Specifications- Numerical Simulation and Experiment," *International Journal of Impact Engineering*, Vol. 32, Nos. 1–4, 2005, pp. 618–630. doi:10.1016/j.ijimpeng.2004.09.001

[11] Klintworth, J. W., and Stronge, W. J., "Elasto-Plastic Yield Limits and Deformation Laws for Transversely Crushed Honeycombs," *International Journal of Mechanical Sciences*, Vol. 30, Nos. 3–4, 1988, pp. 273–292. doi:10.1016/0020-7403(88)90060-4

[12] Papka, S. D., and Kyriakides, S., "In-Plane Compressive Response and Crushing of Honeycomb," *Journal of the Mechanics and Physics of Solids*, Vol. 42, No. 10, 1994, pp. 1499–1532. doi:10.1016/0022-5096(94)90085-X

[13] Honig, A., and Stronge, W. J., "In-Plane Dynamic Crushing of Honeycomb, Part 1: Crush Band Initiation and Wave Trapping," *International Journal of Mechanical Sciences*, Vol. 44, No. 8, 2002, pp. 1665–1696. doi:10.1016/S0020-7403(02)00060-7

[14] Honig, A., and Stronge, W. J., "In-Plane Dynamic Crushing of Honeycomb, Part 2: Application to Impact," *International Journal of Mechanical Sciences*, Vol. 44, No. 8, 2002, pp. 1697–1714. doi:10.1016/S0020-7403(02)00061-9

[15] Chung, J., and Waas, A. M., "Compressive Response of Circular Cell Polycarbonate Honeycombs Under Inplane Biaxial Static and Dynamic Loading, Part 2: Simulations," *International Journal of Impact Engineering*, Vol. 27, No. 10, 2002, pp. 1015–1047. doi:10.1016/S0734-743X(02)00012-X

[16] Olympio, K. R., and Gandhi, F., "Zero-υ Cellular Honeycomb Flexible Skins for One-Dimensional Wing Morphing," *Collection of Technical Papers: 48th AIAA/ASME/ASCE/AHS/ASC Structures, Structural Dynamics, and Materials Conference*, AIAA, Reston, VA, April 2007, pp. 374–401.

[17] Hibbitt, H. D., "ABAQUS/EPGEN: A General Purpose Finite Element Code with Emphasis on Nonlinear Applications," *Nuclear Engineering and Design*, Vol. 77, No. 3, 1984, pp. 271–297. doi:10.1016/0029-5493(84)90106-7

[18] Thorton, P. H., Mahmood, H. F., and Magee, C. L., "Energy Absorption by Structural Collapse," *Structural Crashworthiness*, edited by M. Jones and T. Wierzbicki, Butterworths, London, 1983, p. 97.

[19] Ezra, A. A., and Fay, R. J., "An Assessment of Energy Absorbing Devices for Prospective Use in Aircraft Impact Situations," *Dynamic Response of Structures*, edited by G. Herrmann and N. Perrone, Pergamon, New York, 1971, p. 226.

F. Pai
Associate Editor